

# Callosal fiber length scales with brain size according to functional lateralization, evolution, and development

Liyuan Yang<sup>1</sup>, Chenxi Zhao<sup>1</sup>, Yirong Xiong<sup>1</sup>, Suyu Zhong<sup>1</sup>, Di Wu<sup>1</sup>, Shaoling Peng<sup>1</sup>, Michel Thiebaut de Schotten<sup>2, 3</sup>, Gaolang Gong<sup>1, 4, 5\*</sup>

<sup>1</sup> State Key Laboratory of Cognitive Neuroscience and Learning & IDG/McGovern Institute for Brain Research, Beijing Normal University, Beijing, China

<sup>2</sup> Brain Connectivity and Behaviour Laboratory, Sorbonne Universities, Paris, France

<sup>3</sup> Groupe d'Imagerie Neurofonctionnelle, Institut des Maladies Neurodégénératives-UMR 5293, CNRS, CEA, University of Bordeaux, Bordeaux, France

<sup>4</sup> Beijing Key Laboratory of Brain Imaging and Connectomics, Beijing Normal University, Beijing, China

<sup>5</sup> Chinese Institute for Brain Research, Beijing, China

**Running title:** Callosal fiber length scaling

## \* Correspondence:

Dr. Gaolang Gong

National Key Laboratory of Cognitive Neuroscience and Learning & IDG/McGovern Institute for Brain Research, Beijing Normal University,  
#19 Xijiekouwai Street, Beijing 100875, China

Tel: +86 10 58804678; Fax: +86 10 58804678

E-mail: [gaolang.gong@bnu.edu.cn](mailto:gaolang.gong@bnu.edu.cn)

## Abstract

Brain size significantly impacts the organization of white matter fibers. Fiber length scaling – the degree to which fiber length varies according to brain size – was overlooked. We investigated how fiber lengths within the corpus callosum, the most prominent white matter tract, vary according to brain size. The results showed substantial variation in length scaling among callosal fibers, replicated in two large healthy cohorts (~2000 individuals). The underscaled callosal fibers mainly connected the precentral gyrus and parietal cortices, whereas the overscaled callosal fibers mainly connected the prefrontal cortices. The variation in such length scaling was biologically meaningful: larger scaling corresponded to larger neurite density index but smaller fractional anisotropy values; cortical regions connected by the callosal fibers with larger scaling were more lateralized functionally as well as phylogenetically and ontogenetically more recent than their counterparts. These findings highlight an interaction between interhemispheric communication and organizational and adaptive principles underlying brain development and evolution.

**Keywords:** corpus callosum, brain size, fiber length scaling, fiber composition, functional lateralization, cortical expansion, diffusion MRI

# Introduction

Total brain size varies dramatically across evolution, development, and individuals. Large brains' structures are not simple linearly scaled versions of small brains, e.g., cortical expansion of large brains is disproportionately larger for higher cognitive function regions<sup>1,2</sup>. The scaling patterns of specific brain structures provide essential clues for understanding organizational and adaptive principles underlying brain development and evolution<sup>3–5</sup>.

An increase in brain size also has a significant impact on brain circuits<sup>6</sup>. In larger brains, fiber length is inevitably increased, accompanied by a longer delay in conduction and slower information transfer. It is well known that brain fibers can increase their myelination and diameter to increase conduction velocity and compensate for this delay<sup>7,8</sup>. These adaptations, however, cannot apply systematically to all fiber tracts due to the limit in brain space and energy consumption<sup>9</sup>, leading to alternative biological strategies that might impact fiber length differently. While the fiber length adjustment to brain size has been assumed uniform so far, heterogeneity in fiber length scaling may reveal adaptive principles underlying brain development and evolution.

In the present study, we assessed whether length scaling variations exist according to brain size within the corpus callosum (CC), the principal white matter (WM) bundle supporting the communication between the two brain hemispheres. We further investigated the relationship between CC length scaling with functional lateralization and cortical evolutionary and developmental expansion.

# Results

The present study used two large neuroimaging datasets, each comprising ~ 1000 healthy subjects, i.e., the Human Connectome Project (HCP)<sup>10</sup> and the UK Biobank (UKB)<sup>11</sup>. High-quality diffusion magnetic resonance imaging (dMRI) was applied to reconstruct callosal fibers virtually. The fiber length scaling variation was then thoroughly analyzed on the entire midsagittal CC (mCC).

Fiber length was extracted for each participant's mCC voxel in both datasets and showed excellent test-retest reproducibility (Figure S1). After aligning individual mCC maps to a standard template, a log-log regression was employed to estimate the CC length scaling coefficients with greater brain size for each mCC voxel, adjusting for age and sex variables.

## Callosal fiber variation in length scaling with brain size

As illustrated in Figure 1, the callosal fiber length scaling coefficients showed substantial variation across mCC voxels. Specifically, the rostrum, genu, anterior body, and posterior splenium showed the largest scaling coefficients, whereas the smallest values were in the posterior body and isthmus parts of the CC. The mCC scaling

coefficient maps estimated from both the HCP and UKB datasets were strikingly similar (Spearman correlation  $r_s = 0.86$ ,  $p < 10^{-4}$ ), indicating excellent reproducibility for such a scaling pattern across the mCC. This observed pattern was also quite robust to the computing methods for voxel-wise fiber length and the selected samples for regression model fitting (Figure S2).

### **Relevance to callosal fiber composition**

To determine whether the length scaling relates to underlying fiber composition, we evaluated the Spearman correlation of the scaling coefficient with two popular dMRI-derived WM microstructural parameters on the mCC: neurite density index (NDI) and fractional anisotropy (FA). Across all mCC voxels, the length scaling coefficients were found to be positively correlated with NDI (HCP:  $r_s = 0.41$ ,  $p < 10^{-4}$ ; UKB:  $r_s = 0.35$ ,  $p < 10^{-4}$ ; Figure 2A) and negatively correlated with FA (HCP:  $r_s = -0.06$ ,  $p = 0.01$ ; UKB:  $r_s = -0.14$ ,  $p < 10^{-4}$ ; Figure 2B). Moreover, we parcellated the mCC into Aboitiz's ten segments, which measured histological fiber density for each of the ten segments<sup>12</sup>. Significant correlation was found between the histological fiber density of callosal fiber  $> 0.4\mu\text{m}$  and NDI ( $r_s = 0.74$ ,  $p = 0.008$ ) but not with FA ( $r_s = 0.12$ ,  $p = 0.36$ ). Across the ten mCC segments, there was no significant correlation between the length scaling coefficient and NDI or FA (Figure 2), possibly due to the limited statistical power.

### **Relevance to cortical functional lateralization**

The length scaling variation between callosal fibers putatively reflected cortical differences in evolutionary or developmental demands for rapid interhemispheric communication, which may have accounted for cortical differences in functional lateralization of the human brain. To assess this hypothesis, we estimated an overall functional lateralization index (LI) across cognitive domains (all 575 cognitive terms in the current Neurosynth database) on the cortical surface (Figure 3A) using a Neurosynth-based meta-analysis<sup>13</sup> (<http://Neurosynth.org>).

For each mCC voxel, we mapped its connected cortical region and calculated its regional mean functional LI. Across all mCC voxels, the length scaling coefficients were positively correlated with the functional LI (HCP:  $r_s = 0.36$ ,  $p < 10^{-4}$ ; UKB:  $r_s = 0.30$ ,  $p < 10^{-4}$ ; Figure 3A). We also observed a positive correlation between length scaling and the functional LI across the ten Aboitiz's segments (HCP:  $r_s = 0.72$ ,  $p = 0.01$ ; UKB:  $r_s = 0.71$ ,  $p = 0.01$ ), indicating the robustness of this correlation. Therefore, stronger cortical functional lateralization was accompanied by greater length scaling of the connected callosal fibers, thus suggesting less demand for rapid cortical interhemispheric communication. At both the voxel and segment levels, the partial Spearman correlations after controlling for the NDI and FA remained significant, indicating an independent relationship between callosal fiber length scaling and functional lateralization (Table S1).

### **Relevance to cortical expansion**

To directly assess its evolutionary and developmental relevance, we investigated

whether the length scaling of callosal fibers was related to the evolutionary and developmental expansion of their connected cortical regions, i.e., i) cortical expansion in humans relative to macaques and ii) cortical expansion in human adults relative to human infants. As described above, we assigned the mean cortical expansion index from the connected cortical region to each mCC voxel/segment. As shown in Figure 3B-C, the mCC patterns of callosal fiber length scaling aligned well with those for the cortical expansion index during evolution (across voxels: HCP,  $r_s = 0.71$ ,  $p < 10^{-4}$ ; UKB,  $r_s = 0.50$ ,  $p < 10^{-4}$ ; across segments: HCP,  $r_s = 0.76$ ,  $p = 0.007$ ; UKB,  $r_s = 0.78$ ,  $p = 0.005$ ) and during development (across voxels: HCP,  $r_s = 0.47$ ,  $p < 10^{-4}$ ; UKB,  $r_s = 0.41$ ,  $p < 10^{-4}$ ; across segments: HCP,  $r_s = 0.71$ ,  $p = 0.01$ ; UKB,  $r_s = 0.65$ ,  $p = 0.02$ ). After controlling for the NDI and FA, the partial Spearman correlations remained significant at the voxel level but were not always significant at the segment level (Table S1). The nonsignificant partial Spearman correlation was likely due to the limited statistical power from the small sample size (i.e., ten segments).

### Callosal fibers of length over-scaling or under-scaling with brain size

Theoretically, a callosal fiber length coefficient of  $1/3$  indicates iso-scaling with brain size. In contrast, coefficients  $> 1/3$  indicate that callosal fiber length scales more with greater brain size (i.e., over-scaling), and coefficients  $< 1/3$  indicate that callosal fiber length scales less with brain size (i.e., under-scaling). As illustrated in Figure 4A, significant mCC clusters (false discovery rate, FDR corrected  $p < 0.05$ ) existed for both over-scaling and under-scaling. The overlapping regions between the clusters from the two datasets were designated as the final clusters; one large cluster exhibited over-scaling, and two small clusters demonstrated under-scaling (Figure 4B). The over-scaling cluster covered most of the anterior half of the mCC, which mainly connects the prefrontal cortices between the two hemispheres. In contrast, the first under-scaling cluster was located on the dorsal splenium, mainly connecting the precuneus and superior parietal lobule; the other under-scaling cluster was on the posterior body, mainly connecting the paracentral lobule and precentral gyrus (Figure 4C).

As shown in Figure 4E, the callosal fibers of over-scaling showed greater NDI value ( $t(777) = 8.8$ ,  $p < 10^{-4}$ ) and smaller FA value ( $t(777) = -9.9$ ,  $p < 10^{-4}$ ), as well as stronger functional lateralization ( $t(8570) = 31.9$ ,  $p < 10^{-4}$ ), larger evolutionary and developmental expansion ( $t(8570) = 70.3$ ,  $p < 10^{-4}$ ;  $t(8570) = 47.4$ ,  $p < 10^{-4}$ ) in their connected cortical regions, compared with the callosal fibers of under-scaling. These results are compatible with the observed correlations of callosal fiber scaling with respect to the fiber composition and cortical measures described above.

Finally, our validation analyses confirmed the minimal influence of the procedure of mapping the cortical topography of mCC voxels or segments on our results presented above (Table S1 and Figure S3).

## Discussion

Our present study revealed substantial variation in length scaling with brain size among

callosal fibers, ranging from under-scaling to iso- scaling to over-scaling, replicated in two large healthy cohorts. Fiber length under-scaling was mainly observed in callosal fibers connecting the precentral gyrus and parietal cortices, whereas over-scaling mainly involved callosal fibers connecting the prefrontal cortices. Notably, the variation in such length scaling was biologically meaningful: the length scaling of callosal fibers significantly correlated with underlying fiber composition, as well as with human functional lateralization, evolutionary and developmental expansion of the fiber-connected cortical regions. Validation analyses confirmed excellent reproducibility and robustness of these observations.

The scaling patterns of specific gray matter (GM) features with brain size have been repeatedly studied, either across species or across human individuals<sup>2,14–16</sup>. In contrast, very few studies have been devoted to the scaling of WM fiber length with brain size, possibly due to technical difficulties in directly measuring fiber length *in vivo* (e.g., requiring 3D fiber reconstruction). Our currently observed length scaling of callosal fibers and its biological relevance proved the overall feasibility and importance of studying WM fibers' length scaling.

Although the absolute length of callosal fibers is increased in larger brains, the substantial variation in length scaling suggests a change in the relative length among callosal fibers. Such length reorganization in larger brains is unlikely confined to the CC but extrapolates to other WM fibers across the entire brain. On the other hand, previous studies have demonstrated fiber diameter/myelination reorganization in larger brains<sup>8,17</sup>. Thus, larger brains choose to jointly adjust the two critical determinants of conduction delay, i.e., fiber diameter/myelination and length, to reach an optimal fiber composition of the entire brain to achieve structural and functional efficacy best. Such a strategy is theoretically advantageous compared to solely adjusting either fiber diameter/myelination or length. The joint adjustment strategy offers a larger search space for the optimal fiber reorganization solution by providing two-parameter dimensions. Notably, the median or mean diameter of callosal fibers did not significantly differ between species or human individuals, although the largest diameter of callosal fibers did increase in species with larger brains<sup>8,18</sup>. Therefore, larger brains seem to adjust the relative length across the CC more than they adjust the fiber diameter/myelination. This particular adjustment model might be specific to the CC, and its underlying mechanisms deserve further investigation.

Callosal fiber density and diameters also exhibited significant variation in the mCC, as revealed by human histology<sup>12</sup>. Callosal fibers with larger diameters mainly connect sensorimotor cortices, and small diameters connect association cortices<sup>19</sup>. This particular pattern reflects functional differences in cross-hemisphere communication among different types of cortical areas; sensorimotor functions require rapid integration of information from the two hemispheres, and higher cognitive functions in association cortices work well with slow interhemispheric information transfer. In the present study, one of our observed under-scaling clusters was around the mCC posterior body, mainly connecting the sensorimotor cortex; the only cluster of over-scaling predominantly connected the prefrontal lobe—the primary association cortex. Therefore, the



requirement of rapid communication between bilateral sensorimotor areas is accomplished by both larger fiber diameter and under-increased fiber length in larger brains. Smaller fiber diameter and an overly increased fiber length contribute to slower interhemispheric communication between bilateral association cortices. The rapid interhemispheric communication for low-level cortices but the slow interhemispheric communication for high-level cortices may reflect a general principle of the functional organization across species and individuals.

The present study used two dMRI parameters to estimate the spatial pattern of mCC fiber composition *in-vivo*. The NDI measures fiber density well on the mCC, and it showed a strong correlation with the influential Aboitiz's histological data for the mCC fiber density<sup>12</sup>. Putatively, lower fiber density comes with a larger local fiber diameter on the mCC. The mCC FA did not correlate with histological fiber density and may reflect the myelination degree<sup>20</sup>. The observed length scaling's positive correlation with NDI and negative correlation with FA suggested that callosal fibers of less length scaling (i.e., smaller increase in fiber length) had lower density, larger diameter, and were myelinated. These empirical pieces of evidence support that smaller increase in fiber length, larger fiber diameter, and increased myelination are simultaneously implemented to jointly facilitate rapid interhemispheric communications of particular cortical regions in larger brains. On the other hand, the association between these callosal fiber characteristics may relate to cost control of fiber reorganization in larger brains: to save physical space and energy consumption, highly myelinated callosal fibers of large diameter tend to minimize their length increase as possible.

Interhemispheric communication efficacy has long been considered a contributing factor to the emergence of functional lateralization. According to Ringo's influential hypothesis, the excessive callosal conduction delay of larger brains leads to functional lateralization during evolution<sup>9</sup>. In contrast, functional lateralization may arise due to inter-hemispheric inhibition through callosal fibers<sup>21</sup>. Measurements of the mCC area or dMRI parameters have been repeatedly used as a proxy for callosal connectivity to test these hypotheses<sup>22,23</sup>, with contrasting results. Both positive and negative correlations between callosal connectivity and functional lateralization have been reported<sup>24,25</sup>, supporting both hypotheses. By directly measuring callosal length, our observations suggested that more scaling of callosal fiber length (i.e., a relatively greater conduction delay in larger brains) is accompanied by stronger functional lateralization, therefore favoring Ringo's hypothesis but not the inhibition hypothesis. Ringo's original hypothesis did specify that an excessive interhemispheric conduction delay, which leads to functional lateralization, is mainly caused by increased callosal fiber length due to brain size expansion. Our observed positive correlation of callosal length scaling with functional lateralization provides more direct support for this influential hypothesis.

The association of the length scaling of callosal fibers with cortical expansion during evolution and postnatal development provides direct support for evolutionary and developmental contributions to scaling variation. For a cortical region, less demand for rapid interhemispheric communication (as reflected by greater length scaling) and

greater expansion of the cortical area are likely rooted in the same motivations for the entire brain's optimal functional efficiency. As revealed previously, expansion of the cortical area across human individuals also showed under-scaling, iso-scaling, over-scaling with greater brain size<sup>2</sup>. The under- and over-expansion of cortical regions with greater brain size were attributed mainly to under- or over- increased cortical folding<sup>26</sup>. Notably, the under- or over-expansion of cortical regions can be achieved by modifying the degree of cortical folding, surface outward degree, or both. Given the U shape of callosal fibers, their length scaling can partly represent their connected cortical regions' outward surface degree. Therefore, the observation of callosal fiber length under- or over-scaling provides evidence for the contributing role of the surface outward degree in under- or over-expansion of the cortical area across individuals or during evolution and development. However, for specific regions, the extent that the changes in cortical folding degree or outward surface degree contribute to the evolutionary and developmental expansion of the cortical area remains elusive.

Despite, biological mechanisms underlying the association of the length scaling with the nontrivial callosal and cortical measures remain unclear. It might relate to the shared genetic or environmental factors. At the neural level, causal relationships could exist among these fiber and cortical characteristics. Animal studies are warranted in the future in order to evaluate these speculations

In conclusion, the current findings of callosal fiber variation in length scaling with brain size provide direct empirical evidence for length reorganization among WM fibers in larger brains. These observations also highlight the interactions of evolutionary and developmental constraints with interhemispheric communication.

## Methods

### Discovery dataset

The discovery dataset included all possible HCP participants for whom both diffusion and T1 images were available. It comprised 928 healthy young adults (female/male: 503/425; age range: 22-37 years). Retest diffusion and T1 imaging data were available on 35 of these subjects (test-retest interval: 1 month - 11 months). Informed consent was obtained from all subjects, and the protocol was approved by the Institutional Review Board of Washington University. MRI scanning was performed using a customized Siemens Connectome Skyra 3T scanner. Diffusion-weighted (DW) images were acquired using a spin-echo echo-planar imaging (EPI) sequence with the following parameters: repetition time (TR) = 5520 ms, echo time (TE) = 89.5 ms, flip angle = 78°, field of view (FOV) = 210 × 180 mm<sup>2</sup>, matrix = 168 × 144, slices = 111, and resolution = 1.25 mm × 1.25 mm × 1.25 mm. Diffusion weightings of b = 0, 1000, 2000, and 3000 s/mm<sup>2</sup> were applied in 18, 90, 90 and 90 directions, respectively. High-resolution 3D T1-weighted (T1W) images were acquired using a magnetization prepared rapid gradient echo (MPRAGE) sequence and the following parameters: TR



= 2400 ms, TE = 2.14 ms, TI = 1000 ms, flip angle = 8°, FOV = 224 × 224 mm<sup>2</sup>, and resolution = 0.7 mm × 0.7 mm × 0.7 mm. DW and T1W images were preprocessed using the HCP minimal preprocessing pipeline<sup>27</sup>.

## Replication dataset

A subset of the UKB dataset was selected as our replication dataset. To maximally match the age range and sample size with the discovery dataset, all UKB participants under the age of 43 years for whom both diffusion and T1 images were available were included in the replication dataset, comprising 981 healthy adults (female/male: 562/419; age range: 40-43 years). Informed consent was obtained from all UKB subjects, and the protocol was approved by the North West Multicenter Research Ethics Committee. MRI data from the UKB sample were acquired using a Siemens Skyra 3T scanner. DW images were acquired using a spin-echo EPI sequence with the following parameters: TR = 3600 ms, TE = 92 ms, flip angle = 78°, FOV = 208 × 208 mm<sup>2</sup>, 72 slices, and resolution = 2 mm × 2 mm × 2 mm. Diffusion weightings of  $b = 0, 1000, 2000$  s/mm<sup>2</sup> were applied in 5, 50, and 50 directions. High-resolution 3D T1WIs were acquired using an MPRAGE sequence and the following parameters: TR = 2000 ms, TE = 2.01 ms, TI = 880 ms, flip angle = 8°, FOV = 256 × 256 mm<sup>2</sup>, and resolution = 1 mm × 1 mm × 1 mm. DW and T1W images were preprocessed using the UKB brain imaging processing pipeline<sup>28</sup>.

## Total brain size

The total brain size was defined as the intracranial volume (ICV). Specifically, the T1W image of each individual was first nonlinearly registered to the Montreal Neurological Institute (MNI) template, and its inverted transform was then used to convert the template ICV mask back to the individual T1W image space. For each individual, the total brain size was calculated as the physical volume of the ICV mask in the native space.

## Individual midsagittal CC (mCC) and its alignment to the template

The HCP minimal preprocessing pipeline aligned the anterior commissure (AC), AC–posterior commissure (PC) line, and interhemispheric plane of the T1W images to the MNI template using a rigid transform of 6 degrees of freedom. This transform maintains the original size and shape of the brain. We applied the same aligning procedure to the T1W images of UKB participants. On the resultant T1W image of each individual, the midsagittal plane's sagittal slice was selected, and the mCC boundary was then manually outlined by a trained rater (D.W). The mCC boundary of 50 randomly selected participants was outlined two weeks later by the rater to assess the manual outlining reliability. The Dice coefficient of the mCC masks ranged from 0.95 to 0.99 (mean: 0.98, STD: 0.009), and the intraclass correlation coefficient (ICC) of the mCC area reached 0.99.

Individual mCC maps were further nonlinearly aligned to the template mCC map in MNI space, i.e., a standard mCC template to ensure comparability of the mCC across individuals. The detailed registration procedure is described in the Supplementary

Methods. For each individual, the mCC alignment was carefully checked by visual inspection.

### **Callosal fiber length**

DMRI tractography was used to extract callosal fiber streamlines passing through the mCC. The detailed procedure is included in the Supplementary Methods. For each mCC voxel, the streamlines passing through it and linking the bilateral cerebral cortex were selected. Their average length was computed as the callosal length value for this voxel. One mCC map of fiber length was obtained for each subject, which was further transformed into the standard mCC template space described above. To evaluate the test-retest reproducibility of the voxel-wise measure for callosal fiber length, we reran the above analyses for the HCP retest subjects. We estimated the voxel-wise ICC of the fiber length measure on the mCC.

### **Length scaling coefficients with brain size**

As was done previously<sup>2</sup>, we estimated the fiber length scaling coefficient with greater brain size using a multiple regression model:  $\log(\text{fiber length}) = \beta * \log(\text{brain size}) + \beta_1 * \text{age} + \beta_2 * \text{sex} + \text{intercept}$ , where the  $\beta$  represents the length scaling coefficient. In the model, age and sex were included as covariates. This regression model fitting was applied to each voxel of the mCC template, resulting in a mCC map for the callosal fiber length scaling coefficient.

Theoretically, if WM fibers' internal geometrical shape is invariant for brain size, the WM fiber length should scale as the 1/3 power of brain size, i.e., iso-scaling. For empirical scaling coefficients, coefficients  $> 1/3$  indicate that the WM fiber length scales more with greater brain size, i.e., over-scaling; coefficients  $< 1/3$  indicate that WM fiber length scales less with brain size, i.e., under-scaling. Each voxel's scaling coefficient on the mCC template was statistically compared to 1/3 to identify the significant clusters with over-scaling or under-scaling. To correct for multiple comparisons, the false discovery rate (FDR) procedure was performed at  $q$  value of 0.05<sup>29</sup>.

### **WM microstructural measures on the mCC**

To measure callosal fiber composition, two widely used dMRI-derived parameters, i.e., neurite density index (NDI) and fractional anisotropy (FA), were estimated for each mCC voxel<sup>30,31</sup>. The mCC maps of NDI and FA were further transformed to the standard mCC template space for each individual. The representative NDI and FA maps in healthy adults were then generated by averaging all HCP individual maps of the template space. Such representative maps were used to assess the relevance of length scaling to callosal fiber composition.

### **Mapping cortical topography of each mCC voxel**

For each HCP subject, the minimal preprocessing pipeline outputted FreeSurfer-generated pial and white surfaces resampled onto the standard 32k\_fs\_LR mesh in the native volume space. Each mCC voxel's streamlines were assigned to their closest

vertex on the white surface within a sphere with a 2-mm radius centered at its endpoint, therefore yielding a standard 32K surface map of streamline counts for this voxel. For each voxel on the mCC template, such a streamline count map on the standard 32K surface was comparable across individuals. The group streamline count surface map was then obtained by averaging the individual streamline count surface maps across all HCP individuals. We applied a threshold to the group streamline count surface map to extract a binary cortical topography map for each mCC voxel. Specifically, the mean + 0.5\*standard deviation (STD) of the group streamline count value across the entire surface was used as the main threshold. To evaluate the influence of such a threshold on the results, we reran relevant analyses by applying the following two thresholds: 1) a less stringent threshold, i.e., the mean of the group streamline count value across the entire surface, and 2) a more stringent threshold, i.e., the mean + 1\*STD of the group streamline count value across the entire surface.

## Cortical measures

To assess the relevance of callosal fibers' length scaling to particular functional and structural aspects of their connected cortical regions, we derived several cortical measures; these measures are described below.

Functional lateralization index: We followed a recent study's methods to estimate the cortical overall functional LI across cognitive domains<sup>25</sup>. First, we selected available cognitive terms (575 in total) in the current Neurosynth database<sup>13</sup> (<http://Neurosynth.org>). We applied the Neurosynth tool for each cognitive term to generate a whole-brain meta-activation image in MNI space. After aligning this meta-activation image to a symmetric image template, we projected the values onto the standard 32k\_fs\_LR mesh in MNI space. For each surface vertex, the absolute between-hemisphere difference of the meta-activation values was calculated as the absolute degree of functional lateralization for this cognitive term. To yield an overall functional LI across all cognitive domains, we simply averaged the individual surface maps of functional lateralization across all 575 cognitive terms.

Evolutionary expansion index: The cortical expansion map in humans relative to macaques was estimated by Hill and colleagues<sup>1</sup>. We adopted the expansion index and resampled the values onto the standard 32k\_fs\_LR surface mesh.

Human developmental expansion index: The cortical expansion map in human adults relative to human infants was estimated by Hill and colleagues<sup>1</sup>. Likewise, we adopted the expansion index and resampled the values onto the standard 32k\_fs\_LR surface mesh.

For each mCC voxel, we assigned the mean value of the aforementioned cortical measure within its connected cortical region, resulting in one mCC map for the cortical functional lateralization, evolutionary, and developmental expansion.

## Statistical analysis

To determine whether the length scaling coefficient was related to callosal

microstructural measures and cortical measures above, we calculated the Spearman correlations across all mCC voxels. We used the Spearman correlation because the length scaling coefficient showed a nonnormal distribution on the mCC. A permutation test (10,000 permutations) was adopted to estimate the Spearman correlation coefficient's statistical significance ( $r_s$ ). To evaluate the robustness and reproducibility of the observed correlation across the analysis resolution of the mCC, we additionally parcellated the entire mCC into ten segments. The parcellation scheme followed an influential mCC study, which measured histological fiber density for each of the ten segments<sup>12</sup>. Likewise, we assigned the mean callosal microstructural measures or the mean cortical index value of the connected cortical region to each mCC segment. We then reran the Spearman correlation analysis across all ten mCC segments.

To examine an independent relationship between callosal fiber length scaling and the aforementioned cortical measures, we reran the Spearman correlations across the mCC voxels or segments described above while controlling for the NDI and FA.

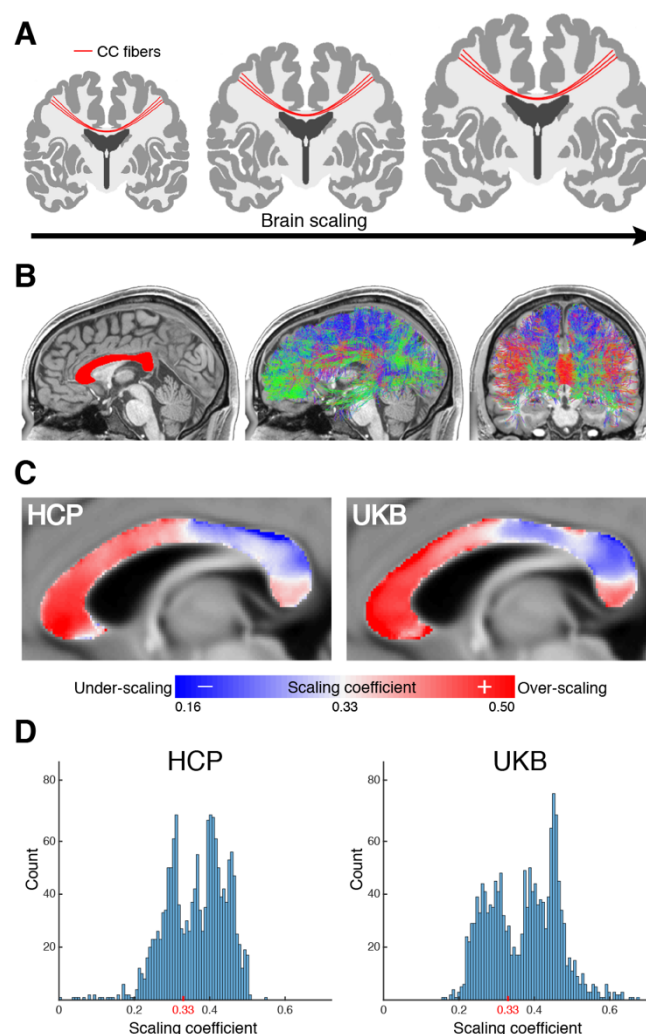


**Figure 1. Callosal fiber variation in length scaling with brain size.** (A) Schematic of callosal fiber length scaling with brain size. (B) The midsagittal CC (red) and callosal fibers from one example subject. (C) Callosal fiber length scaling coefficient maps of the HCP and UKB datasets. (D) The histogram of scaling coefficients. The iso-scaling coefficient 0.33 is highlighted in red.

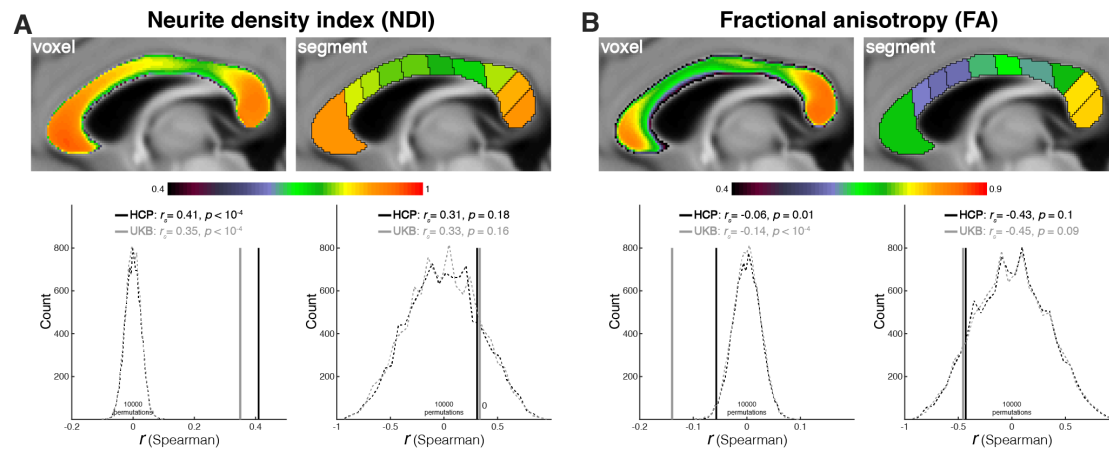


**Figure 2. Relevance to callosal fiber composition.** The relationships between callosal fiber length scaling and neurite density index (A), and fractional anisotropy (B). Top row is the group-averaged neurite density index (NDI) and fractional anisotropy (FA) at the voxel and segment level. Bottom row is the Spearman correlation between the microstructural measures and callosal fiber length scaling coefficient across midsagittal CC voxels and segments. Black: HCP, Gray: UKB. Solid lines represent empirical Spearman correlation coefficients; dashed lines represent the null distribution of Spearman correlation coefficients derived from 10,000 permutations.



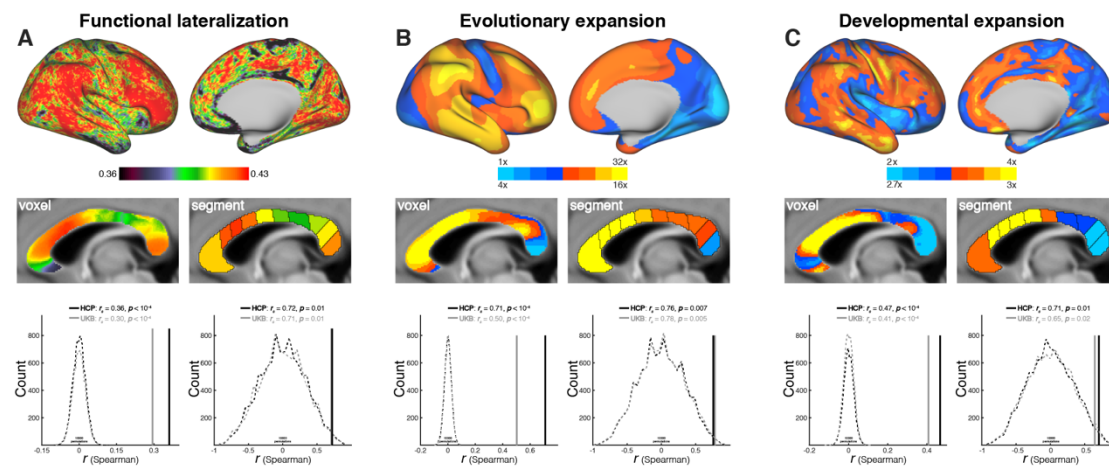


**Figure 3. Relevance to cortical measures.** The relationships between callosal fiber length scaling and cortical functional lateralization (A), the evolutionary cortical expansion of the primate brain (B), and the developmental cortical expansion of the human brain (C). Top row is the averaged cortical functional lateralization map across cognitive terms, evolutionary cortical expansion map, and developmental cortical expansion map. Middle row is the cortical measures of the midsagittal CC at the voxel and segment level. Bottom row is the Spearman correlation between the cortical measures and callosal fiber length scaling coefficient across midsagittal CC voxels and segments. Black: HCP, Gray: UKB. Solid lines represent empirical Spearman correlation coefficients; dashed lines represent the null distribution of Spearman correlation coefficients derived from 10,000 permutations.

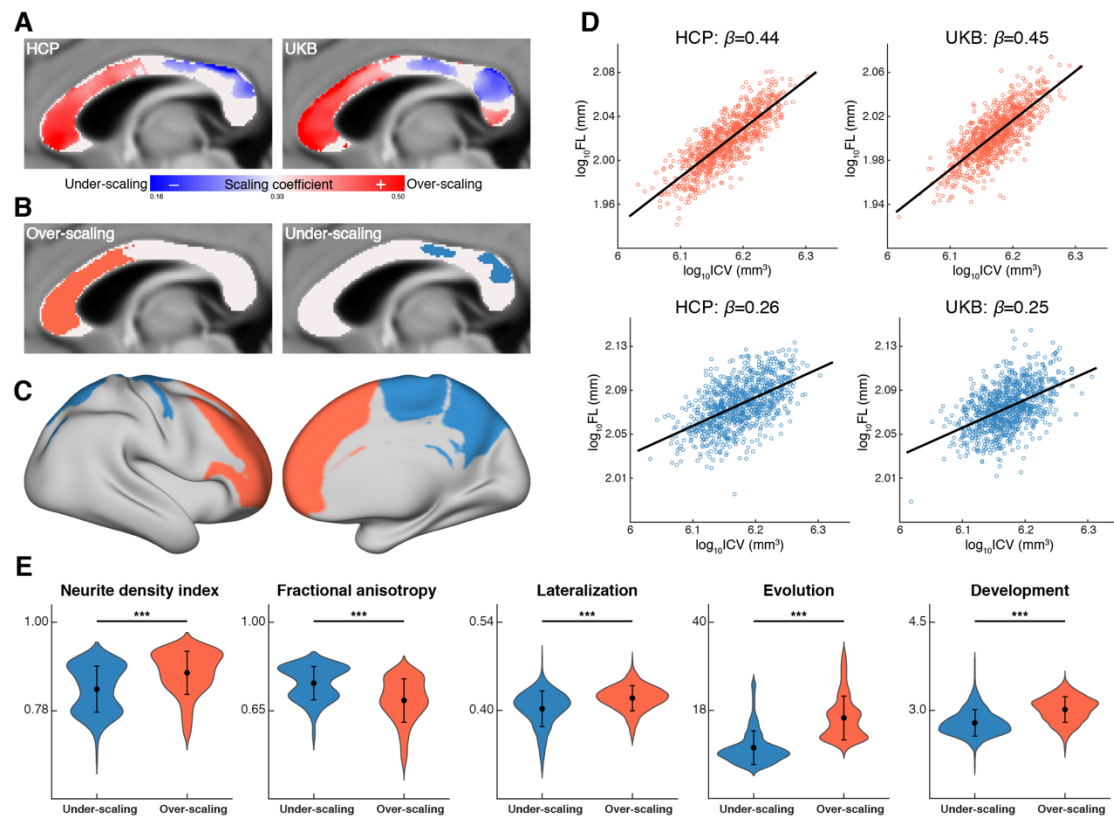


**Figure 4. Callosal fibers of length over-scaling or under-scaling with brain size.** (A) The midsagittal CC areas showing significant fiber length over-scaling or under-scaling. (B) The conjunction midsagittal CC area of length over-scaling or under-scaling between the HCP and UKB datasets. Left panel: over-scaling clusters. Right panel: under-scaling clusters. (C) The cortical regions connected by the callosal fibers passing through the over-scaling and under-scaling clusters. (D) Scatter plots of the logarithm of fiber length and the logarithm of ICV for the over-scaling (i.e., significant  $\beta > 0.33$ ) and under-scaling (i.e., significant  $\beta < 0.33$ ) clusters. (E) The differences between the over-scaling and under-scaling clusters in the two white matter microstructural measures and three cortical measures above. The mean (black dot) and standard deviation are overlaid on the violin map. \*\*\*:  $p < 0.001$ . Orange: over-scaling clusters. Blue: under-scaling clusters.

## Data availability

The datasets analysed during the current study are available at <https://www.humanconnectome.org/> and <https://www.ukbiobank.ac.uk/>. In addition, processed data are available on request to the corresponding author [gaolang.gong@bnu.edu.cn](mailto:gaolang.gong@bnu.edu.cn).

## Code availability

The code used in the following analyses is available on request to the corresponding author [gaolang.gong@bnu.edu.cn](mailto:gaolang.gong@bnu.edu.cn).

## Reference

1. Hill, J. *et al.* Similar patterns of cortical expansion during human development and evolution. *Proc Natl Acad Sci U S A* **107**, 13135–13140 (2010).
2. Reardon, P. K. *et al.* Normative brain size variation and brain shape diversity in humans. *Science* **360**, 1222–1227 (2018).
3. Zhang, K. & Sejnowski, T. J. A universal scaling law between gray matter and white matter of cerebral cortex. *Proc Natl Acad Sci U S A* **97**, 5621–5626 (2000).
4. Herculano-Houzel, S., Mota, B., Wong, P. & Kaas, J. H. Connectivity-driven white matter scaling and folding in primate cerebral cortex. *Proc Natl Acad Sci U S A* **107**, 19008–19013 (2010).
5. Van Essen, D. C. Scaling of human brain size. *Science* **360**, 1184–1185 (2018).
6. Kaas, J. H. Why is Brain Size so Important: Design Problems and Solutions as Neocortex Gets Bigger or Smaller. *Brain and Mind* **1**, 7–23 (2000).
7. Waxman, S. G., Kocsis, J. D. & Stys, P. K. *The axon: structure, function, and pathophysiology*. (Oxford University Press, USA, 1995).
8. Wang, S. S.-H. *et al.* Functional trade-offs in white matter axonal scaling. *J Neurosci* **28**, 4047–4056 (2008).
9. Ringo, J. L., Doty, R. W., Demeter, S. & Simard, P. Y. Time is of the essence: a conjecture that hemispheric specialization arises from interhemispheric conduction delay. *Cereb Cortex* **4**, 331–343 (1994).
10. Van Essen, D. C. *et al.* The Human Connectome Project: a data acquisition perspective. *Neuroimage* **62**, 2222–2231 (2012).
11. Miller, K. L. *et al.* Multimodal population brain imaging in the UK Biobank prospective epidemiological study. *Nature neuroscience* **19**, 1523–1536 (2016).
12. Aboitiz, F., Scheibel, A. B., Fisher, R. S. & Zaidel, E. Fiber composition of the human corpus callosum. *Brain Res* **598**, 143–153 (1992).
13. Yarkoni, T., Poldrack, R. A., Nichols, T. E., Van Essen, D. C. & Wager, T. D. Large-scale automated synthesis of human functional neuroimaging data. *Nature Methods* **8**, 665–670 (2011).
14. Im, K. *et al.* Brain size and cortical structure in the adult human brain. *Cereb Cortex* **18**, 2181–2191 (2008).
15. Herculano-Houzel, S. The remarkable, yet not extraordinary, human brain as a

- scaled-up primate brain and its associated cost. *Proc Natl Acad Sci U S A* **109** Suppl 1, 10661–10668 (2012).
16. Mota, B. & Herculano-Houzel, S. BRAIN STRUCTURE. Cortical folding scales universally with surface area and thickness, not number of neurons. *Science* **349**, 74–77 (2015).
  17. Phillips, K. A. *et al.* The corpus callosum in primates: processing speed of axons and the evolution of hemispheric asymmetry. *Proc Biol Sci* **282**, 20151535 (2015).
  18. Olivares, R., Montiel, J. & Aboitiz, F. Species differences and similarities in the fine structure of the mammalian corpus callosum. *Brain Behav Evol* **57**, 98–105 (2001).
  19. Caminiti, R. *et al.* Diameter, length, speed, and conduction delay of callosal axons in macaque monkeys and humans: comparing data from histology and magnetic resonance imaging diffusion tractography. *J Neurosci* **33**, 14501–14511 (2013).
  20. Chang, E. H. *et al.* The role of myelination in measures of white matter integrity: Combination of diffusion tensor imaging and two-photon microscopy of CLARITY intact brains. *Neuroimage* **147**, 253–261 (2017).
  21. Cook, N. D. Homotopic callosal inhibition. *Brain and Language* **23**, 116–125 (1984).
  22. Bloom, J. S. & Hynd, G. W. The role of the corpus callosum in interhemispheric transfer of information: excitation or inhibition? *Neuropsychol Rev* **15**, 59–71 (2005).
  23. van der Knaap, L. J. & van der Ham, I. J. M. How does the corpus callosum mediate interhemispheric transfer? A review. *Behav Brain Res* **223**, 211–221 (2011).
  24. Josse, G., Seghier, M. L., Kherif, F. & Price, C. J. Explaining function with anatomy: language lateralization and corpus callosum size. *J Neurosci* **28**, 14132–14139 (2008).
  25. Karolis, V. R., Corbetta, M. & Thiebaut de Schotten, M. The architecture of functional lateralisation and its relationship to callosal connectivity in the human brain. *Nat Commun* **10**, 1417 (2019).
  26. Zilles, K., Palomero-Gallagher, N. & Amunts, K. Development of cortical folding during evolution and ontogeny. *Trends Neurosci* **36**, 275–284 (2013).
  27. Glasser, M. F. *et al.* The minimal preprocessing pipelines for the Human Connectome Project. *Neuroimage* **80**, 105–124 (2013).
  28. Alfaro-Almagro, F. *et al.* Image processing and Quality Control for the first 10,000 brain imaging datasets from UK Biobank. *Neuroimage* **166**, 400–424 (2018).
  29. Genovese, C. R., Lazar, N. A. & Nichols, T. Thresholding of statistical maps in functional neuroimaging using the false discovery rate. *Neuroimage* **15**, 870–878 (2002).
  30. Basser, P. J., Mattiello, J. & LeBihan, D. Estimation of the effective self-diffusion tensor from the NMR spin echo. *J Magn Reson B* **103**, 247–254 (1994).
  31. Zhang, H., Schneider, T., Wheeler-Kingshott, C. A. & Alexander, D. C. NODDI: Practical in vivo neurite orientation dispersion and density imaging of the human brain. *NeuroImage* **61**, 1000–1016 (2012).

## **Acknowledgements**

We thank Yanchao Bi for valuable discussions. This work was supported by the National Science Foundation of China [82021004, 81671772, G.G.]. Michel Thiebaut de Schotten has received funding from the European Research Council (ERC) under the European Union's Horizon 2020 research and innovation programme (grant agreement no. 818521). Data were provided by the Human Connectome Project, WU-Minn Consortium (Principal Investigators: David Van Essen and Kamil Ugurbil; 1U54MH091657) funded by the 16 NIH Institutes and Centers that support the NIH Blueprint for Neuroscience Research; and by the McDonnell Center for Systems Neuroscience at Washington University. UK Biobank brain imaging was funded by the UK Medical Research Council and the Wellcome Trust.

## **Author contributions**

G.G. designed and coordinated the research. L.Y. performed the research. L.Y., C.Z., Y.X., S.Z., D.W., and S.P. analyzed the data. L.Y., M.T.d.S., and G.G. interpreted the outcomes. L.Y., M.T.d.S., and G.G. wrote the manuscript, which was edited by all authors.

## **Competing interests**

The authors declare no competing interests.